CERN-PH-TH/2004-016

The running of the electromagnetic coupling α in small-angle Bhabha scattering

A.B. Arbuzov
BLTP, Joint Institute for Nuclear Research, Dubna, 141980, Russia

D. Haidt
DESY, Notkestrasse 85, D-22603 Hamburg, Germany

C. Matteuzzi M. Paganoni
Dipartimento di Fisica, Università di Milano-Bicocca
and
INFN-Milano, Piazza della Scienza 3, I-20126 Milan, Italy

L. Trentadue*
Department of Physics, CERN Theory Division, 1211 Geneva 23, Switzerland

Abstract

A method to determine the running of α from a measurement of small-angle Bhabha scattering is proposed and worked out. The method is suited to high statistics experiments at e^+e^-colliders, which are equipped with luminometers in the appropriate angular region. A new simulation code predicting small-angle Bhabha scattering is also presented.

*On leave from Dipartimento di Fisica, Università di Parma and INFN, Gruppo Collegato di Parma, I-43100 Parma, Italy

1 Introduction

The electroweak Standard Model $SU(2) \otimes U(1)$ contains Quantum Electrodynamics (QED) as a constitutive part. The running of the electromagnetic coupling α is determined by the theory as

$$\alpha(q^2) = \frac{\alpha(0)}{1 - \Delta\alpha(q^2)}, \tag{1}$$

where $\alpha(0) = \alpha_0$ is the Sommerfeld fine structure constant, which has been measured to a precision of 3.7×10^{-9} [1]; $\Delta\alpha(q^2)$ positive arises from loop contributions to the photon propagator. The numerical prediction of electroweak observables involves the knowledge of $\alpha(q^2)$, usually for $q^2 \neq 0$. For instance, the knowledge of $\alpha(m_Z^2)$ is relevant to the evaluation of quantities measured by the LEP experiments. This is achieved by evolving α from $q^2 = 0$ up to the Z-mass scale $q^2 = m_Z^2$. The evolution expressed by the quantity $\Delta\alpha$ receives contributions from leptons, hadrons and the gauge bosons. The hadronic contribution to the vacuum polarization, which cannot be calculated from first principles, is estimated with the help of a dispersion integral and evaluated [2] by using total cross section measurements of $e^+e^- \rightarrow$ hadrons at low energies. Therefore, any evolved value $\alpha(q^2)$ particularly for $|q^2| > 4m_\pi^2$, is affected by uncertainties originating from hadronic contributions. The uncertainty on $\alpha(m_Z^2)^{-1}$ induced by these data is as small as ± 0.09 [2]; nevertheless it turned out [3] that this limits the accurate prediction of electroweak quantities within the Standard Model, particularly for the prediction of the Higgs mass.

While waiting for improved measurements from BEPC, VEPP-4M and DAFNE as input to the dispersion integral, intense efforts are made to improve on estimating the hadronic shift $\Delta\alpha_{\rm had}$, as for instance [4] - [7], and to find alternative ways of measuring α itself. Attempts have been made to measure $\alpha(q^2)$ directly, using e^+e^- data at various energies, such as measuring the ratio of $e^+e^-\gamma/e^+e^-$ [8] or more directly the angular distribution of Bhabha scattering [9].

In this article the running of α is studied using small-angle Bhabha scattering. This process provides unique information on the QED coupling constant α at low *space-like* momentum transfer $t = -|q^2|$, where

$$t = -\frac{1}{2}\ s\ (1 - \cos\theta) \tag{2}$$

is related to the total invariant energy $\sqrt{s}$ and to the scattering angle θ of the final-state electron. The small-angle region has the virtue of giving access to values of $\alpha(t)$ without being affected by weak contributions. The cross section can be theoretically calculated with a precision at the per mille level. It is dominated by the photonic t channel exchange and the non-QED contributions have been computed [10] and are of the order of 10^{-4} (see table 1); in particular, contributions from boxes with two weak bosons are safely negligible.

In general, the Bhabha cross section is computed (see sect. 3) from the entire set of gauge-invariant amplitudes in both the s and t channels. Consequently, two invariant scales s and t govern the process. The different amplitudes are functions of both s and t and also the QED coupling α appears as $\alpha(s)$ resp. $\alpha(t)$ [11]. However, the restriction of Bhabha scattering to the kinematic regime of small angles results in a considerable simplification, since the s channel then gives only a negligible contribution, as is quantitatively demonstrated in table 1. Thus, the measurement of the angular distribution allows us indeed to verify directly the running of the coupling $\alpha(t)$. For the actual calculations, $\theta \gg m_e/E_{\rm beam}$ and $E_{\rm beam} \gg m_e$ must be satisfied (see sect. 4.1). Obviously, in order to manifest the running, the experimental precision must be adequate.

This idea can be realized by high-statistics experiments at e^+e^- colliders equipped with finely segmented luminometers, in particular by the LEP experiments, given their large event samples, by SLC and future Linear Colliders. The relevant luminometers cover the t-range from a few GeV^2 to order 100 GeV^2.

The t-dependence of the quantity $\Delta\alpha(t)$ (eqs. 1, 2) at small values of t is illustrated in fig. 1. It shows the predicted running of α in the relevant space-like region. The figure is obtained using the program *alphaQED* by Jegerlehner [2]. At low energies (see fig. 2) $\Delta\alpha$ is dominated by the contribution

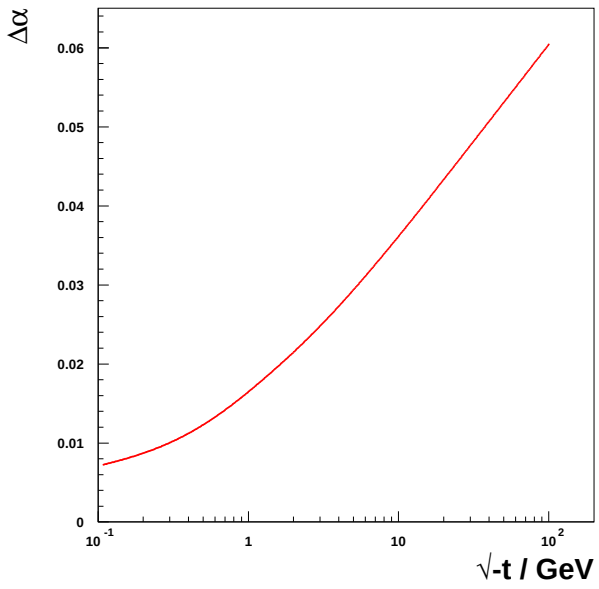

Figure 1: $\Delta\alpha$ *versus* $\sqrt{-t}$ *in units of GeV in the space-like region.*

from the leptons, while with increasing energy also the contribution involving hadrons gets relevant. The region where hadronic corrections are critical is contained in the considered t-range.

2 The method

The experimental determination of the angular distribution of the Bhabha cross section requires the precise definition of a Bhabha event in the detector. The analysis follows closely the procedure adopted in the luminosity measurement, which is described in detail, for instance in ref. [12], and elaborates on the additional aspect related to the measurement of a differential quantity. To this aim the luminosity detector must have a sufficiently large angular acceptance and adequate fine segmentation. The variable t (eq. 2) is reconstructed on an event-by-event basis.

The method to measure the running of α exploits the fact that the cross section for the process $e^+e^- \to e^+e^-$ can be conveniently decomposed into three factors :

$$\frac{\mathrm{d}\sigma}{\mathrm{d}t} = \frac{\mathrm{d}\sigma^0}{\mathrm{d}t}\left(\frac{\alpha(t)}{\alpha(0)}\right)^2 (1+\Delta r(t)) \tag{3}$$

as worked out in sect. 3. All three factors are predicted to a precision of 0.1% or better. The first factor on the right-hand side refers to the effective Bhabha Born cross section, including soft and virtual photons according to ref. [10], which is precisely known, and accounts for the strongest dependence on t. The vacuum-polarization effect in the leading photon t channel exchange is incorporated in the running of α and gives rise to the squared factor in eq. 3. The third factor, $\Delta r(t)$, collects all the remaining real (in particular collinear) and virtual radiative effects not incorporated in the running of α. The experimental data after correction for detector effects have to be compared with eq. 3. The t dependence is rather steep, thus migration effects may need attention.

This goal is achieved by using a newly developed program based on the already existing semianalytical code `NLLBHA` [10, 13]. A detailed description of this code called `SAMBHA` is given in sect.4.

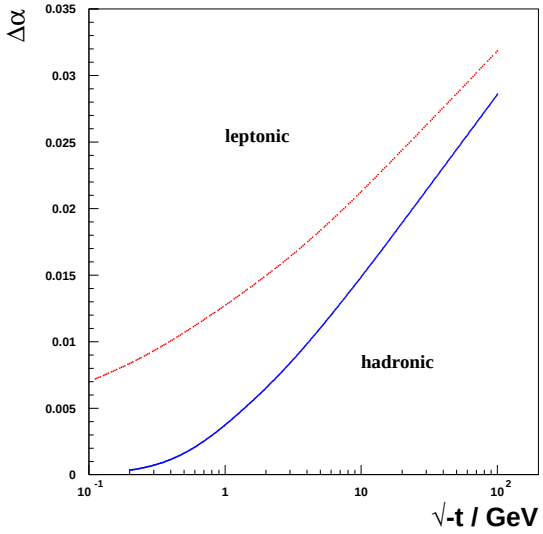

Figure 2: *Contributions to $\Delta\alpha$ from leptons (dashed curve) and hadrons (solid curve) versus $\sqrt{-t}$ in units of GeV.*

3 Theory

It is convenient to confront the fully corrected measured cross section with the Bhabha cross section, including radiative corrections in the factorized form given by eq. 3. The physical cross section is infrared safe [10]. This decomposition is neither unique nor dictated by a compelling physical reason; rather it allows the separation of the different sources of t dependence in a transparent way without introducing any additional theoretical uncertainty. The various factors are discussed one by one in the following subsections.

3.1 The cross section $\mathrm{d}\sigma^0/\mathrm{d}t$

The differential cross section $\mathrm{d}\sigma^0/\mathrm{d}t$ is defined as :

$$\frac{\mathrm{d}\sigma^0}{\mathrm{d}t} = \frac{\mathrm{d}\sigma^B}{\mathrm{d}t}\left(\frac{\alpha(0)}{\alpha(t)}\right)^2 . \tag{4}$$

The factor $d\sigma^B/dt$ is the Bhabha cross section in the improved Born approximation, which, by definition, includes the running of α. As seen explicitly in the formulae below (eq. 5) the term $\alpha(t)/\alpha(0)$ is not factorized completely in the improved Born cross section. In order to have the factorized form of eq. 3 the t channel contribution to the running of α has been taken out. In this way, $\mathrm{d}\sigma^0/\mathrm{d}t$ contains not only the usual Born t dependence, i.e. $1/t$, but also some weaker t dependences arising from s channel amplitudes with vacuum polarization effects taken into account [10], although numerically small as mentioned above.

The improved Born cross section for Bhabha scattering within the electroweak Standard Model is precisely known (see refs. [14, 15, 16]). The differential cross section $\mathrm{d}\sigma^B/\mathrm{d}t$ differs from $\mathrm{d}\sigma^0/\mathrm{d}t$ by the inclusion of those radiative corrections that affect only the propagator of the exchanged photon. They form a gauge-invariant subset of all radiative corrections and are shown explicitly. It is convenient to decompose $\mathrm{d}\sigma^B/\mathrm{d}t$ into the contributions arising from the t channel (B_t), the s channel (B_s) and

their interference (B_i):

$$\frac{\mathrm{d}\sigma^B}{\mathrm{d}t} \;=\; \frac{\pi\alpha_0^2}{2s^2}\mathrm{Re}\big\{B_t + B_s + B_i\big\}, \tag{5}$$

where

$$\begin{aligned}
B_t &= \left(\frac{s}{t}\right)^2\left\{\frac{5+2c+c^2}{(1-\Pi(t))^2} + \xi\frac{2(g_v^2+g_a^2)(5+2c+c^2)}{(1-\Pi(t))}\right.\\
&+ \left.\xi^2\Big(4(g_v^2+g_a^2)^2 + (1+c)^2(g_v^4+g_a^4+6g_v^2g_a^2)\Big)\right\}\\
B_s &= \frac{2(1+c^2)}{|1-\Pi(s)|^2} + 2\chi\frac{(1-c)^2(g_v^2-g_a^2)+(1+c)^2(g_v^2+g_a^2)}{1-\Pi(s)}\\
&+ \chi^2\big[(1-c)^2(g_v^2-g_a^2)^2 + (1+c)^2(g_v^4+g_a^4+6g_v^2g_a^2)\big]\\
B_i &= 2\frac{s}{t}(1+c)^2\left\{\frac{1}{(1-\Pi(t))(1-\Pi(s))}\right.\\
&+ (g_v^2+g_a^2)\left(\frac{\xi}{1-\Pi(s)} + \frac{\chi}{1-\Pi(t)}\right)\\
&+ \left.(g_v^4+6g_v^2g_a^2+g_a^4)\xi\chi\right\}
\end{aligned}$$

$$\begin{aligned}
\chi &= \frac{s}{s-m_z^2+im_Z\Gamma_Z}\cdot\frac{1}{\sin 2\theta_w}\\
\xi &= \frac{t}{t-m_Z^2}\cdot\frac{1}{\sin 2\theta_w},\\
g_a &= -\frac{1}{2}, \quad g_v = -\frac{1}{2} + 2\sin^2\theta_w),\\
t &= (p_1-q_1)^2 = -\frac{1}{2}\,s\,(1-c),\\
c &= \cos\theta, \qquad \theta = \widehat{\boldsymbol{p}_1\boldsymbol{q}_1}.
\end{aligned}$$

Here s is the total squared invariant mass, θ_w the electroweak mixing angle and θ the scattering angle between the initial and final electron with momentum $\boldsymbol{p}_1$ and $\boldsymbol{q}_1$ respectively (see ref. [10]).

In table 1 the cross sections are given in nanobarns for the pure QED and electroweak cases. QED_t denotes the contribution of the t channel pure QED Feynman diagrams. The cross sections are integrated over two relevant angular ranges. The table shows that the t channel photon exchange dominates the cross section at small angles and justifies why the process is suited for investigating the t dependence, and so the running of $\alpha(t)$.

By comparing the values of the electroweak cross section with the pure QED one, it is seen that the Z-boson exchange gives a negligible contribution to small-angle scattering. In the last two lines ($\mathrm{EW{+}VP}_t$ and EW+VP) there are numbers for the cross section with vacuum polarization taken into account in the t channel only, and in all channels, correspondingly. One can see that the effect of s channel vacuum polarization is small, as a result of the smallness of the s channel photon–exchange contribution itself. The last line in the table corresponds to the complete formula in eq. 5.

3.2 The running of α

In eq. 5 the two-point functions $\Pi(t) = \Delta\alpha(t)$ and $\Pi(s) = \Delta\alpha(s)$ are responsible for the running of α in the space-like and time-like regions. In the language of Feynman diagrams the effect arises from

Table 1: Various cross sections in nb as a function of the centre-of- mass energy in GeV integrated over the two angular ranges 45–110 mrad and 5–50 mrad. The index t denotes the contribution of the corresponding t channel Feynman diagrams alone. The last columns are of interest for furture Linear Colliders.

$\sqrt{s}$ (GeV)	91.187	91.2	189	206	500	1000	3000
	45 mrad $<\ \theta\ <$ 110 mrad						
$\sqrt{\langle -t \rangle}$ (GeV)	3.4	3.4	7.1	7.7	18.8	37.5	112.6
QED	51.428	51.413	11.971	10.077	1.7105	0.42763	0.047514
QED_t	51.484	51.469	11.984	10.088	1.7124	0.42809	0.047566
EW	51.436	51.413	11.965	10.072	1.7105	0.42871	0.049507
EW+VP_t	54.041	54.018	12.743	10.745	1.8590	0.47303	0.055748
EW+VP	54.036	54.013	12.742	10.744	1.8588	0.47296	0.055742
	5 mrad $<\ \theta\ <$ 50 mrad						
$\sqrt{\langle -t \rangle}$ (GeV)	1.1	1.1	2.2	2.4	5.8	11.6	34.8
QED	4963.4	4962.0	1155.4	972.54	165.08	41.271	4.5857
QED_t	4963.5	4962.1	1155.4	972.57	165.09	41.272	4.5858
EW	4963.4	4962.0	1155.4	972.53	165.08	41.272	4.5885
EW+VP_t	5075.0	5073.5	1190.6	1003.3	172.51	43.647	4.9603
EW+VP	5075.0	5073.5	1190.6	1003.3	172.51	43.646	4.9605

fermion-loop insertions into the virtual photon lines:

$$\begin{aligned}\Pi(t) &= \frac{\alpha_0}{\pi}\left(\delta_t + \frac{1}{3}L - \frac{5}{9}\right) \\ &+ \left(\frac{\alpha_0}{\pi}\right)^2\left(\frac{1}{4}\,L + \zeta(3) - \frac{5}{24}\right) \\ &+ \left(\frac{\alpha_0}{\pi}\right)^3\Pi^{(3)}(t) + \mathcal{O}\left(\frac{m_e^2}{t}\right),\end{aligned}$$

where

$$L = \ln\frac{Q^2}{m_e^2}, \qquad Q^2 = -t, \qquad \zeta(3) = 1.202$$

and where the leading part of the two-loop contribution to the polarization operator is taken into account. The most significant part arises from the electrons and is $L/3 - 5/9$.

The $\mathcal{O}(\alpha)$ and $\mathcal{O}(\alpha^2)$ leptonic vacuum polarization has been known for many years [17]. The third-order (three–loop) leptonic contributions $\Pi^{(3)}(t)$ have recently been calculated [18]. In the Standard Model, δ_t contains contributions from muons, τ-leptons, W-bosons and hadrons :

$$\begin{aligned}\delta_t &= \delta_t^\mu + \delta_t^\tau + \delta_t^W + \delta_t^H, \\ \delta_s &= \delta_t\ (t \to s),\end{aligned}$$

which means that δ_s is obtained from δ_t by substituting s by t, see ref. [10]. The contributions from

the leptons ($l = \mu, \tau$) and from the W are theoretically calculable and given by:

$$\begin{aligned}
\delta_t^l &= \frac{1}{2}\, v_l \left(1 - \frac{1}{3} v_l^2\right) \ln \frac{v_l + 1}{v_l - 1} + \frac{1}{3}\, v_l^2 - \frac{8}{9} \\
v_l &= \sqrt{1 + \frac{4m_l^2}{Q^2}}\,, \\
\delta_t^W &= \frac{1}{4}\, v_W\, (v_W^2 - 4) \ln \frac{v_W + 1}{v_W - 1} - \frac{1}{2}\, v_W^2 + \frac{11}{6} \\
v_W &= \sqrt{1 + \frac{4M_W^2}{Q^2}}\,.
\end{aligned}$$

For $Q^2 \gg m_l^2$ the formula simplifies to

$$\delta_t^l = \frac{1}{3} \ln \frac{Q^2}{m_l^2} - \frac{5}{9},$$

The hadronic contribution cannot be calculated theoretically; instead, it can be expressed as a dispersion integral involving experimentally measured e^+e^- cross sections:

$$\delta_t^{\rm had} = \frac{Q^2}{4\pi\alpha_0^2} \int\limits_{4m_\pi^2}^{\infty} \frac{\sigma^{e^+e^- \to {\rm h}}\,(s')}{s' + Q^2}\, {\rm d}s'. \tag{6}$$

For numerical calculations, hadronic contributions as included in the parametrisation of refs. [4, 19] are adopted.

This procedure, as usually assumed (see e.g. [5]), is based on the analyticity of the function $\alpha(q^2)$ in the complex plane, except possibly at the energies corresponding to the Landau pole. For the leptonic contributions $\delta_{s,t}^{e,\mu,\tau}$ this assertion is true, while for the hadronic contribution $\delta_t^{\rm had}$ it relies on the dispersion approach to the entire, non-perturbative, hadronic physics (see eq. 6). This ends up in a single analytical function that can be used to deal with the vacuum polarization in the t channel.

3.3 The radiative factor $1 + \Delta r(t)$ and neglected terms

For the present investigation of the small-angle Bhabha cross section only the corrections consistently needed to maintain the required accuracy are kept. All these corrections are included in the new code `SAMBHA`. All the following contributions have been proved to be negligible [10] and are dropped :

- Any electroweak effect beyond the tree level, for instance appearing in boxes or vertices with Z^0 and W bosons, running weak coupling, etc.
- Box diagrams at order α^2 and larger
- Contributions of order α^2 without large logarithms, leading from order α^4 (i.e. $\alpha^4 L^4$, $\cdots$) and subleading higher order ($\alpha^3 L^2$, $\alpha^4 L^3$, $\cdots$)
- Contributions from pair-produced hadrons, muons, taus and the corresponding virtual pair corrections to the vertices (estimated to be of the order of $0.5{\times}10^{-4}$).

The radiatively corrected Bhabha cross section is denoted by ${\rm d}\sigma/{\rm d}t$. Numerically it differs from ${\rm d}\sigma^B/{\rm d}t$ by less than a few per cent for small angles, depending on energy and final-state selection procedure.

4 Monte Carlo codes and comparison

The precise determination of the luminosity at e^+e^- colliders is a crucial ingredient to obtain an accurate evaluation of all the physically relevant cross sections. They necessarily have to rely on some reference process, which is usually taken to be the small-angle Bhabha scattering. Given the high statistical precision provided by the LEP collider, an equally precise knowledge of the theoretical small-angle Bhabha cross section is mandatory. In the 1990's the substantial progress in measuring the luminosity reached by the LEP machine has prompted several groups to make a theoretical effort aiming at a 0.1% accuracy [12, 20]. This goal has indeed been achieved by developing a dedicated strategy. For the first time small-angle Bhabha scattering was evaluated analytically, following a new calculation technique [10] that yields the required precision. Analytical calculations have been combined with Monte Carlo programs in order to simulate realistically the conditions of the LEP experiments.

The analytical results evaluated for the various contributions to the observed Bhabha cross section in ref. [10], were implemented into the semi–analytical code `NLLBHA` (for a short write–up see in ref. [13]). The important feature of this code consists in the systematic account of all QED radiative corrections required to reach the *per mille* precision. On the other hand, the simulation of realistic experimental acceptances can only be achieved with Monte Carlo techniques. For this purpose a Monte Carlo code, `LABSMC`, was developed [21, 22, 23].

4.1 `SAMBHA-NLLBHA`

The program `LABSMC`, which was intended to describe large-angle Bhabha scattering at high energies, has been complemented with a set of routines from `NLLBHA` so as to be applicable to small-angle Bhabha scattering. This implied the insertion of the relevant second-order next–to–leading radiative corrections ($\mathcal{O}(\alpha^2 L)$) in the Monte Carlo code[1], which are crucial to achieve the per mille accuracy. The extension to cover small angles resulted in the new code `SAMBHA` containing the previously existing features together with the following new characteristics :

- the complete electroweak matrix element at the Born level;
- the complete set of $\mathcal{O}(\alpha)$ QED radiative corrections (including radiation from amplitudes with Z-boson exchange);
- vacuum-polarization corrections by leptons, hadrons [19], and W-bosons;
- 1–loop electroweak radiative corrections and effective EW couplings by means of the `DIZET v.6.30` [24] package;
- higher-order leading-logarithm photonic corrections by means of the electron structure functions [25, 26, 27, 28];
- light pair corrections in the $\mathcal{O}(\alpha^2 L^2)$ leading-logarithm approximation including (optionally) the two-photon and singlet mechanisms.

The code is applicable with the following restrictions:

a) $E_{\rm beam} \gg m_e$: the energy has to be much larger than the electron mass;

b) $m_e/E_{\rm beam} \ll \theta$: extemely small angles are not described well, but the condition is fulfilled in practice for both small- and large-angle Bhabha measurements in the experiments at LEP, SLC and NLC;

c) starting from the second order in α, real photon emission is integrated over, i.e. events with two photons separated from electrons are not generated.

[1]The codes are available upon request from the authors.

4.2 BHLUMI

The Monte Carlo Program BHLUMI which has been used in the LEP analyses, is described in detail in ref. [29].

4.3 Comparison between BHLUMI and SAMBHA

BHLUMI is compared with SAMBHA for integral and, for the first time, also differential distributions. The actual measurements are of calorimetric type. Therefore, event samples are generated with both programs, subjecting each event to a common set of calorimeter-like criteria (hereafter called CALO).

In a first test the program codes were applied to the conditions established by the working group *Event generators for Bhabha scattering* [12], with the result that all numbers were reproduced within the quoted accuracy.

In a further test, about 10^8 Bhabha events were generated according to the calorimeter like conditions specified in sect. 5.1. This selection rejects a considerable part of events with real hard photon radiation. Therefore, the effect of mutual cancellation between virtual and real radiation is suppressed, which inevitably causes fairly large t-dependent radiative corrections. The comparison is made quantitative in the form of the ratio

$$\rho(t) = \frac{\mathrm{d}\sigma_{\mathrm{sambha}}/\mathrm{d}t - \mathrm{d}\sigma_{\mathrm{bhlumi}}/\mathrm{d}t}{\mathrm{d}\sigma_{\mathrm{bhlumi}}/\mathrm{d}t}$$

and displayed in fig. 3. A linear logarithmic fit to the cross-section ratios and their statistical uncertainties gives

$$\rho(t) = -(0.0039 \pm 0.0002) - (0.0046 \pm 0.0010)\ \log\frac{-t}{\langle -t\rangle}$$

with $\langle t\rangle = -8.3 GeV^2$.

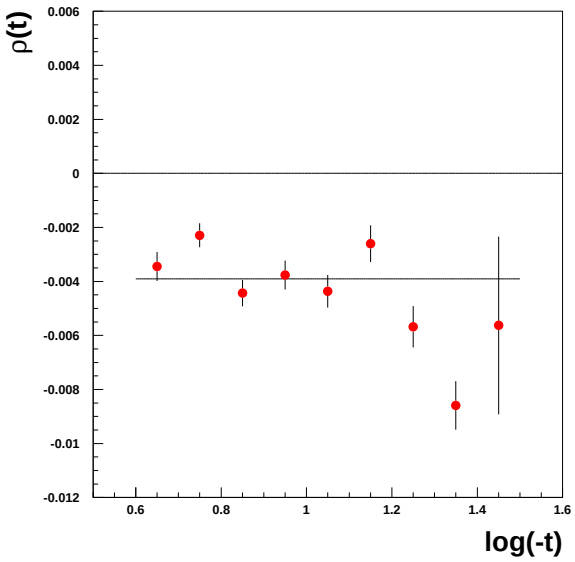

Figure 3: *Cross section ratio $\rho(t)$ as a function of log $(-t)$, with t in units of GeV^2 .*

The two programs differ significantly, on average by 0.4%. At the present level of investigation, it cannot be excluded that there is a weak t dependence.

It is not so surprising to find a discrepancy for the differential quantity, while getting good agreement for the integral quantity. In fact, the key element is the far stronger restriction in the event selection for the two cases. In the integral case the events are accepted over the entire angular range of the luminometer, while for the differential analysis the same selection criteria are applied to a set of segments covering eventually the full range of the luminometer. This implies that an event accepted in the integral case is not necessarily accepted in the differential one owing to the more restrictive conditions, so that the sum of events accepted in the segmented luminometer is smaller than the number of events in the full luminometer.

Table 2: Comparison between the codes `NLLBHA` (`SAMBHA`) and `BHLUMI`. Numbers are obtained by using conditions on table 19 in ref. [12]. The relative ratio $\delta r/r$ in per mille is defined by (YR-NOW)/YR. Last column gives the relative difference between `BHLUMI`(NOW) and `SAMBHA`(NOW).

cut	BHLUMI (YR)	BHLUMI (NOW)	δr/r	NLLBHA (YR)	NLLBHA (NOW)	δr/r	
0.1	166.892	166.879	0.07	166.948	166.923	0.14	−0.26
0.3	165.374	165.438	−0.38	165.448	165.420	0.16	0.10
0.5	162.530	162.616	−0.52	162.561	162.25	1.91	2.25
0.7	155.668	155.733	−0.41	155.607	155.40	1.33	2.13
0.9	137.342	137.425	−0.60	137.199	137.32	−0.88	0.76

For a quantitative understanding of this qualitative argument, a selection of events is presented as a function of the cut $s \cdot x_c = s \cdot x_1 x_2$, where x_i is the fractional energy carried by the electron (or positron) (see table 2). Obviously, a value for x_c near to 1 selects configurations with small acollinearity, as opposed to cases with smaller x_c, which favour larger acollinearity configurations. For a given opening angle, events with large acollinearity are hardly accepted; in other words the size of the cone opening angle defines the number of radiative events containing real emitted photons accepted or rejected. Consequently a larger or smaller final-state phase space is probed. Since virtual radiative contributions are unaffected by phase-space restrictions, the interplay between real and virtual radiative contributions strongly depends on the acceptance. The accuracy to which radiative corrections have to be treated becomes crucial.

With the tight cuts required for the study of a differential quantity, as in the case investigated here, fine detailed aspects related to radiative contributions are necessarily probed. Therefore such studies open a new level of comparison between theory and experiment.

5 Evaluation of the running in a simulated experiment

Anticipating the application of the proposed method to measure the t dependence of $\alpha(t)$ on the data of a real experiment, a Monte Carlo simulation is carried out instead, in order to demonstrate the feasibility. An event sample is generated in the conditions of the DELPHI experiment using the existing program `BHLUMI`. In the next subsection the sample so obtained is confronted with the expectation of the new program `SAMBHA`. It should be noted that the t dependence of $\alpha(t)$, i.e. the quantity to be investigated, is stronger by about an order of magnitude than the possible differences in the intrinsic t dependences between `BHLUMI` and `SAMBHA`(see sect.4.3).

5.1 Event generation

The DELPHI detector and its performance are described in ref. [30]. For the analysis, the relevant subdetector is the electromagnetic calorimeter STIC [30], which covers the extreme forward and

backward directions. It has a ring structure with segmentation in both θ and ϕ covering $\sqrt{-t}$ ranges from 1.5 to 6 GeV for LEP1 energies and 3 to 12 GeV for LEP2 energies.

Electrons, positrons and photons are observed as clusters. Their reconstruction is based on a cluster algorithm. The Bhabha events are characterized by two narrow high energy electromagnetic clusters opposite to each other and well inside the detector. The cluster algorithm is applied to the observed energy depositions in the cells of the electromagnetic calorimeter. Furthermore, the cluster with the highest energy satifies the more restrictive requirement to be at the radial position R between 10 and 25 cm such as to cause no inefficiency for the opposite cluster.

A Monte Carlo simulation has been performed using `BHLUMI` for three centre-of-mass energies of LEP: 91.2 (Z peak), 189 and 200 GeV. Assuming integrated luminosities $\int \mathcal{L}dt$ typical of the LEP experiments, the number of events passing the selection criteria is obtained and listed in table 3. An event is attributed to ring i, if the highest energy cluster is reconstructed in this ring and the criteria listed below are satisfied.

- Cluster reconstruction:
  The main criterion for merging adjacent cells is:

$$\left(\frac{\Delta\theta}{30\,\mathrm{mrad}}\right)^2 + \left(\frac{\Delta\phi}{870\ \mathrm{mrad}}\right)^2 < 1$$

  where the cluster centre is calculated as the energy-weighted cell centres.

- Only the highest energy cluster in each hemisphere (referred to as *F(forward)* and *B(backward)*) is considered

- Energy requirements:
  $\min(E_F,E_B) > 0.65\ E_{\mathrm{beam}}$
  $\max(E_F,E_B) > 0.94\ E_{\mathrm{beam}}$
  This implies that the Bhabha events have not suffered from sizeable initial-state radiation effects.

- Geometrical acceptance:
  The radial position R of the two opposite clusters must satisfy

$$7\,\mathrm{cm} < R_F, R_B < 28\,\mathrm{cm}$$

- Kinematics:
  The cluster centre and the nominal interaction point of the colliding e^+e^- beams determine the dip angle θ. The quantity t is calculated from the dip angle θ and the nominal centre-of-mass energy $\sqrt{s} = 2E_{\mathrm{beam}}$ according to

$$t = -\frac{1}{2}s(1 - \cos\theta_{\mathrm{max}})$$

  where θ_{max} is defined to be the dip angle of the cluster with the highest energy.

The result of the Monte Carlo experiment is summarized in table 3. Ring 1 and ring 7 have been disregarded in order to exclude any inefficiency from border effects.

5.2 Comparison and evaluation

In this subsection the relevant observables and the parameters to be extracted are established and discussed.

Each ring defines with its boundaries a bin $(t_{\mathrm{min}}, t_{\mathrm{max}})$. The event numbers are to be equated to the corresponding theoretical prediction obtained from the formulae implemented in the program

Table 3: Numbers of events generated with BHLUMI

$\sqrt{s}$(GeV)	91.2	189	200
$\int \mathcal{L}\mathrm{d}t$ (pb^{-1})	75	150	200
Ring 2	1844850	863571	1028210
Ring 3	907754	425586	506131
Ring 4	513696	240550	286994
Ring 5	313218	146731	174740
Ring 6	201893	94033	112168

SAMBHA. In order to extract the t dependence of $\alpha(t)$, eq. 3 is evaluated for each ring R_i defined by the geometry of the DELPHI luminometer. Equation 3 then reads, for ring i :

$$\sigma_i = \sigma_i^0 \left(\frac{\alpha(t_i)}{\alpha(0)}\right)^2 (1+\Delta r_i), \tag{7}$$

with the following definitions :

$$\begin{aligned}
\sigma_i &= \int^{R_i} \mathrm{d}t \frac{\mathrm{d}\sigma}{\mathrm{d}t} \\
\sigma_i^0 &= \int^{R_i} \mathrm{d}t \frac{\mathrm{d}\sigma^0}{\mathrm{d}t} \\
\left(\frac{\alpha(t_i)}{\alpha(0)}\right)^2 &= \int^{R_i} \frac{\mathrm{d}t}{t_{\max}-t_{\min}} \left(\frac{\alpha(t)}{\alpha(0)}\right)^2, \\
1+\Delta r_i &= \left(\frac{\alpha(0)}{\alpha(t_i)}\right)^2 \frac{\sigma_i}{\sigma_i^0}
\end{aligned}$$

Table 4 contains the resulting theoretical values.

Putting together the experimental and theoretical ingredients, i.e. the observed number of events N_i in each ring, together with the relevant luminosities $\int \mathcal{L}\mathrm{d}t$ (from table 3) and σ_i^0, Δr_i (from table 4), we obtain the final formula:

$$\left(\frac{\alpha(t_i)}{\alpha(0)}\right)^2 = \frac{N_i}{\sigma_i^0 \int \mathcal{L}\mathrm{d}t} \frac{1}{1+\Delta r_i}, \tag{8}$$

which can be exploited in a linear fit to access the parameters defining the t dependence of α :

$$\left(\frac{\alpha(t)}{\alpha(0)}\right)^2 = (u_0 \pm \delta u_0) + (u_1 \pm \delta u_1) \cdot \log \frac{-t}{\langle -t \rangle} \tag{9}$$

The parameters of the fit are listed in table 5.

6 Discussion

Table 5 demonstrates that for the case of the DELPHI setup (see sect. 5) and assuming typical integrated luminosities, the statistical accuracy is sufficient to verify the running of α for each of the three centre-of-mass energies.

Equation 8 can be expanded in terms of $\Delta\alpha$ (see eq. 1). It is convenient to consider

$$\frac{N_i}{\sigma_i^0} \frac{1}{1+\Delta r_i} = n_0 + n_1 \log \frac{-t_i}{\langle -t \rangle} \tag{10}$$

Table 4: Theoretical predictions for each ring of the three factors of eq. 7. For the conditions defined in sect. 5.1 the angular boundary of ring i is θ_i=arctan (7+3(i-1))/220).

No. of ring	1	2	3	4	5	6	7
	$\sqrt{s} = 91.2$ GeV						
σ_i^0	63.077	24.728	12.170	6.8694	4.2517	2.8120	1.9552
$\left(\alpha(t_i)/\alpha(0)\right)^2$	1.0425	1.0475	1.0516	1.0551	1.0582	1.0609	1.0634
$1+\Delta r_i$	0.9426	0.9440	0.9412	0.9395	0.9240	0.8915	0.7982
	$\sqrt{s} = 189$ GeV						
σ_i^0	14.685	5.7563	2.8324	1.5984	0.9889	0.6537	0.4542
$\left(\alpha(t_i)/\alpha(0)\right)^2$	1.0554	1.0613	1.0661	1.0702	1.0736	1.0767	1.0794
$1+\Delta r_i$	0.9377	0.9390	0.9360	0.9329	0.9165	0.8858	0.7898
	$\sqrt{s} = 200$ GeV						
σ_i^0	13.115	5.1406	2.5295	1.4274	0.8831	0.5838	0.4057
$\left(\alpha(t_i)/\alpha(0)\right)^2$	1.0565	1.0625	1.0673	1.0714	1.0749	1.0780	1.0807
$1+\Delta r_i$	0.9376	0.9387	0.9352	0.9330	0.9158	0.8847	0.7896
	$\sqrt{s} = 1000$ GeV						
σ_i^0	0.5248	0.2059	0.1014	0.0573	0.0356	0.0236	0.0165
$\left(\alpha(t_i)/\alpha(0)\right)^2$	1.0921	1.0994	1.1050	1.1096	1.1135	1.1169	1.1199
$1+\Delta r_i$	0.8622	0.8620	0.8590	0.8545	0.8398	0.8084	0.7205
	$\sqrt{s} = 3000$ GeV						
σ_i^0	0.0590	0.0234	0.0117	0.0067	0.0042	0.0028	0.0020
$\left(\alpha(t_i)/\alpha(0)\right)^2$	1.1192	1.1267	1.1325	1.1373	1.1414	1.1448	1.1479
$1+\Delta r_i$	0.8467	0.8457	0.8422	0.8381	0.8253	0.7956	0.6975

rather than eq. 8, since in practice the integrated luminosity $\int \mathcal{L}\mathrm{d}t$ is not known. The two coefficients n_0 and n_1 are obtained from a linear fit and contain the information on both the data and theory. Their interpretation is :

$$\begin{aligned} n_0 &= \int \mathcal{L}\mathrm{d}t \cdot \Big(1 + 2\Delta\alpha(\langle t\rangle)\Big) \\ n_1 &= \int \mathcal{L}\mathrm{d}t \cdot \Big(\frac{\mathrm{d}}{\mathrm{d}\log(-t)} 2\Delta\alpha(t)\Big). \end{aligned}$$

The dependence on the integrated luminosity is given explicitly: obviously, one has $n_i = u_i \cdot \int \mathcal{L}\mathrm{d}t$ by comparing eqs. 8, 9,10.

In the ratio n_1/n_0 the dependence of the integrated luminosity drops out :

$$\frac{\mathrm{d}}{\mathrm{d}\log(-t)}\Delta\alpha = \frac{n_1}{2n_0}\Big(1 + 2\Delta\alpha(\langle t\rangle)\Big)$$

The slope $\mathrm{d}\Delta\alpha/\mathrm{d}\log(-t)$, the quantity of interest, is then directly given by the ratio of the two experimentally measured quantities n_0 and n_1, namely $n_1/2n_0$. The contribution of $2\Delta\alpha(\langle t\rangle)$ is small with respect to 1 and can be neglected. The accuracy of the slope is determined by $\delta n_1/2n_0$, i.e. about 10% (see table 5), which is far smaller than the absolute value of $n_1/2n_0$.

Table 5: Table of fit results; the uncertainties δu_0 and δu_1 are uncorrelated.

$\sqrt{s}$	91.2 GeV	189 GeV	200 GeV
u_0	1.0573±0.0005	1.0698±0.0008	1.0703±0.0007
u_1	0.0242±0.0028	0.0284±0.0041	0.0318±0.0038
$\langle -t \rangle$	8.5 GeV^2	36.6 GeV^2	40.9 GeV^2

On the other hand, n_0 relates the integrated luminosity to $\Delta\alpha$ at the average value of t

$$\int \mathcal{L} \mathrm{d}t = \frac{n_0}{1 + 2\Delta\alpha(\langle t \rangle)}$$

Making use of $\Delta\alpha(\langle t \rangle)$ as a priori knowledge the fitted n_0 can be used to derive the integrated luminosity, which is the standard procedure. The statistical precision is given by $\delta n_0/n_0$, which is of the order of 10^{-3}.

In addition, the hadronic contribution to $\Delta\alpha(t)$ (see fig. 2) may be deduced by subtracting the leptonic contribution, which is theoretically known precisely. The extraction of the hadronic contribution is only limited by the experimental precision.

7 Conclusions

A novel approach to access directly and to measure the running of α in the space-like region is proposed. It consists in analysing small-angle Bhabha scattering. Depending on the particular angular detector coverage and on the energy of the beams, it allows a sizeable range of the t variable to be covered.

The feasibility of the method has been put in evidence by the use of a new tool, `SAMBHA` , to calculate the small-angle Bhabha differential cross section with a theoretical accuracy of better than 0.1%.

The information obtained in the t channel can be compared with the existing results of the s channel measurements. This represents a complementary approach, which is direct, transparent and based only on QED interactions and furthermore free of some of the drawbacks inherent in the s channel methods.

The method outlined can be readily applied to the experiments at LEP and SLC. It can also be exploited by future e^+e^- colliders as well as by existing lower energy machines.

An extremely precise measurement of the QED running coupling $\Delta\alpha(t)$ for small values of t may be envisaged with a dedicated luminometer even at low machine energies.

Acknowledgements

We are grateful to the CERN and DESY directorates and to the Universities of Parma and Milan for the hospitality and the support extended to us during the course of this work. Two of us (A.A. and L.T.) want to acknowledge the INTAS Organization for support at early stages of this work. One of us (L.T.) wants to thank the INFN and the Italian Ministry for University and Scientific and Technological Research (MURST) for financial support. We are indebted to Marco Incagli, Graziano Venanzoni and Carlos Wagner for the invitation to present part of these results at the WIN02 Conference and the Sighad03 Workshop. We enjoyed a fruitful discussion with P.M. Zerwas.

References

[1] D.E. Groom et al.: Eur. Phys. J. **C15** (2000) 1

[2] S. Eidelman and F. Jegerlehner: Z. Phys. **C67** (1995) 602

[3] K. Hagiwara, D. Haidt, S. Matsumoto and C.S. Kim: Z. Phys. **C64** (1994) 559;
(ibidem)**C68** (1995) 353;
K. Hagiwara, D. Haidt and S. Matsumoto: Eur. Phys. J. **C2** (1998) 95

[4] F. Jegerlehner: hep-ph/0308117

[5] M. Davier and A. Höcker: Phys. Lett. **B435** (1998) 427;
M. Davier, S. Eidelman, A. Höcker and Z. Zhang: Eur. Phys. J. **C27** (2003) 497

[6] D. Karlen and H. Burkhardt: Eur. Phys. J. **C22** (2001) 39; hep-ex/0105065 (2001)

[7] A.A. Pankov and N. Paver, Eur. Phys. J. **C29** (2003) 313

[8] TOPAZ Collaboration, I. Levine et al.: Phys. Rev. Lett. **78** (1997) 424

[9] L3 Collaboration, M. Acciarri et al.: Phys. Lett. **B476** (2000) 48

[10] A.B. Arbuzov, V.S. Fadin, E.A. Kuraev, L.N. Lipatov, N.P. Merenkov and L. Trentadue, *Small-angle electron-positron scattering with a per mille accuracy*, Nucl. Phys. **B485** (1997) 457.

[11] S.J. Brodsky, G.P. Lepage and P.B.Mackenzie: Phys. Rev. **D28** (1983) 228

[12] LEP Working Group (Convenors S. Jadach and O. Nicrosini): Event Generators
for Bhabha scattering, CERN Report 96-01, p. 229

[13] CERN Report 96-01: NLLBHA short write-up

[14] R. Budny: Phys. Lett. **B55** (1975) 227

[15] D. Bardin, W. Hollik and T. Riemann: Z. Phys. **C49** (1991) 485

[16] M. Böhm, A. Denner and W. Hollik: Nucl. Phys. **B304** (1988) 687

[17] G. Källén and A. Sabry: K. Dan. Vidensk. Selsk. Mat.-Fis. Medd. **29** (1955) No. 17.

[18] M. Steinhauser: Phys. Lett. **B429** (1998) 158

[19] S. Eidelman and F. Jegerlehner: Z. Phys. **C67** (1995) 585

[20] A. Arbuzov et al.: Phys. Lett. **B383** (1996) 238

[21] A.B. Arbuzov: *LABSMC: Monte Carlo event generator for large-angle Bhabha scattering,*
hep-ph/9907298.

[22] A.B. Arbuzov: *Event generation of large-angle Bhabha scattering at LEP2 energies,*
hep-ph/9910280.

[23] M. Kobel et al.:*Two-fermion production in e^+e^- collisions,* hep-ph/0007180,
CERN Report 2000-09-D, p. 115.

[24] D.Y. Bardin, M.S. Bilenkii, T. Riemann, M. Sachwitz and H. Vogt:
Comput. Phys. Commun. **59** (1990) 303

[25] E.A. Kuraev and V.S. Fadin: Sov. J. Nucl. Phys. **41** (1985) 466.

[26] O. Nicrosini and L. Trentadue: Phys. Lett. **B196** (1987) 551; Z. Phys. **C39** (1988) 479

[27] M. Skrzypek: Acta Phys. Polon. **B23** (1992) 135

[28] A.B. Arbuzov: Phys. Lett. **B470** (1999) 252

[29] S. Jadach et al.: Comput. Phys. Commun. **102** (1997) 229

[30] P. Abreu et al.: Nucl. Instr. Meth. **A 378** (1996) 57